

# Molecular-orbital decomposition of the ionization continuum for a diatomic molecule by angle- and energy-resolved photoelectron spectroscopy.

## I. Formalism

Hongkun Park and Richard N. Zare

*Department of Chemistry, Stanford University, Stanford, California 94305*

(Received 19 September 1995; accepted 12 December 1995)

A theoretical formalism is developed for the quantum-state-specific photoelectron angular distributions (PADs) from the direct photoionization of a diatomic molecule in which both the ionizing state and the state of the ion follow Hund's case (b) coupling. The formalism is based on the molecular-orbital decomposition of the ionization continuum and therefore fully incorporates the molecular nature of the photoelectron-ion scattering within the independent electron approximation. The resulting expression for the quantum-state-specific PADs is dependent on two distinct types of dynamical quantities, one that pertains only to the ionization continuum and the other that depends both on the ionizing state and the ionization continuum. Specifically, the electronic dipole-moment matrix element  $r_{l\lambda} \exp(i\eta_{l\lambda})$  for the ejection of a photoelectron with orbital angular momentum quantum number  $l$  making a projection  $\lambda$  on the internuclear axis is expressed as  $\sum_{\alpha_\lambda} \bar{U}_{l\alpha_\lambda}^\lambda \exp(i\pi\bar{\tau}_{\alpha_\lambda}^\lambda) M_{\alpha_\lambda}^\lambda$ , where  $\bar{U}^\lambda$  is the electronic transformation matrix,  $\bar{\tau}_{\alpha_\lambda}^\lambda$  is the scattering phase shift associated with the  $\alpha_\lambda$ th continuum molecular orbital, and  $M_{\alpha_\lambda}^\lambda$  is the real electronic dipole-moment matrix element that connects the ionizing orbital to the  $\alpha_\lambda$ th continuum molecular orbital. Because  $\bar{U}^\lambda$  and  $\bar{\tau}_{\alpha_\lambda}^\lambda$  depend only on the dynamics in the ionization continuum, this formalism allows maximal exploitation of the commonality between photoionization processes from different ionizing states. It also makes possible the direct experimental investigation of scattering matrices for the photoelectron-ion scattering and thus the dynamics in the ionization continuum by studying the quantum-state-specific PADs, as illustrated in the companion article on the photoionization of NO. © 1996 American Institute of Physics. [S0021-9606(96)00611-2]

## I. INTRODUCTION

Recent advances in theoretical and experimental techniques have enabled the dynamical study of molecular photoionization processes in unprecedented detail. Differential photoionization cross sections can now be calculated for small molecules almost quantitatively using *ab initio* methods.<sup>1,2</sup> The development of experimental techniques has allowed for the resolution of individual quantum levels of the molecular ion<sup>3-7</sup> as well as the photoelectron angular distributions (PADs) associated with them.<sup>8-13</sup> The synergy between these theoretical and experimental developments has significantly increased our knowledge about the photoionization of molecules and has narrowed the gap between our understanding of molecular and atomic photoionization.

Perhaps the best example that illustrates the experimental progress in the dynamical study of molecular photoionization is the previous report of a complete quantum mechanical description for the photoionization of the NO  $A^2\Sigma^+(\nu=0)$  state using angle- and energy-resolved photoelectron spectroscopy.<sup>10-12</sup> By ionizing optically aligned NO  $A^2\Sigma^+(\nu=0)$  molecules in a specific quantum level using resonance-enhanced multiphoton ionization (REMPI) and by measuring the PADs associated with the production of each rotational level of the NO<sup>+</sup>  $X^1\Sigma^+(\nu^+=0)$  ion, investigators have been able to deduce all the dynamical parameters needed to describe the photoionization process from the NO  $A^2\Sigma^+(\nu=0)$  state. The dynamical parameters, which are the

electronic dipole-moment matrix elements that connect the NO  $A^2\Sigma^+(\nu=0)$  state to each partial wave in the ionization continuum that yields the NO<sup>+</sup>  $X^1\Sigma^+(\nu^+=0)$  ion, provide a most detailed description of this process and can also be directly compared with the corresponding quantities that are computed in *ab initio* calculations.<sup>14</sup> Although the above procedure has been applied so far only to the photoionization of the NO  $A^2\Sigma^+$  state, it should be generally applicable to the study of photoionization dynamics of other small diatomic molecules.

In the one-photon ionization of a diatomic molecule, the ionization continuum that consists of a photoelectron and the molecular ion in a given rovibronic state is coupled to an ionizing state through the dipolar interaction between the molecule and the ionizing photon (in the limit of low ionization intensity). Therefore, the same final state is reached in the photoionization from different ionizing states when the photoelectron energy and the rovibronic state of the molecular ion are the same. Despite this commonality between different photoionization pathways, the dipole-moment matrix elements formulated based on the partial-wave decomposition of the molecular ionization continuum pertain only to a photoionization event from a given ionizing state and do not give detailed insight into the dynamics of the ionization continuum. This situation is in contrast to that in atomic photoionization, in which the relationship between dipole-moment matrix elements for distinct photoionization processes has

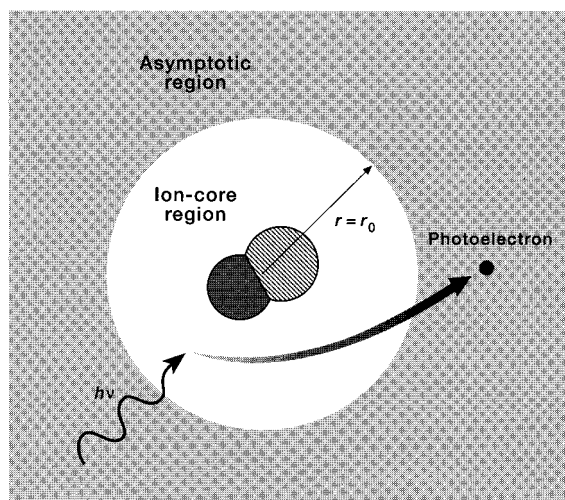


FIG. 1. A schematic illustration of the photoionization of a diatomic molecule. In the figure  $r_0$  designates a radial distance from the center of mass of the ion core to a (fictitious) surface that divides the ion-core region and the asymptotic region.

been used to provide a unified description of the ionization continuum of an atom.<sup>15–22</sup> Because the ionic potential under which the photoelectron moves is a central field within the independent electron approximation, the partial-wave channels, each denoted by a definite electronic orbital angular momentum  $l$ , form a complete set of independent ionization channels in atomic photoionization. Consequently, the phase difference between dipole-moment matrix elements for different partial-wave channels remains the same for photoionization processes from different electronic states of an atom. The phase difference is in essence a characteristic of the ionization continuum of an atom, not the atomic energy level from which photoionization occurs.

When the photoelectron is far from the ion core, whether the ion core is atomic or molecular, it moves principally under the influence of the Coulombic potential because of the charge on the ion core (see Fig. 1).<sup>23</sup> This region of the configuration space where the Coulombic potential dominates the photoelectron motion is designated as the *asymptotic region*. Because of the central nature of the Coulombic potential, the partial-wave description of the ionization continuum is appropriate in the asymptotic region. On the other hand, the photoelectron feels the nature of the ionic core when it is near the core, which we call the *ion-core region*.<sup>24</sup> The dynamics of the photoelectron in this region is what differentiates the atomic and the molecular ionization continua. When the ion core is atomic, the photoelectron moves under the central potential within the independent electron approximation, although the potential is different from the Coulombic one because of the shielding caused by the presence of other electrons. When the ion core is molecular, the potential under which the photoelectron moves is noncentral even in the independent electron approximation, and the description of the ionization continuum based on partial waves with definite  $l$  is not appropriate in the ion-core region.

The separation of the electronic configuration space into the ion-core region and the asymptotic region is justified because any multipolar potential that the photoelectron experiences falls much faster with distance than the Coulombic potential. The multipolar interaction can thus be considered to be short range as long as the ion-core region is large enough to encompass a region of the photoelectron configuration space where the bulk of multipolar interactions occur. Because the ion-core region should be large, however, the interaction between the photoelectron and the ion-core is not uniform even inside the ion-core region, and the interaction can be classified into two distinct types depending on the distance between the photoelectron and the ion core.<sup>25,26</sup> When the photoelectron is inside the ion-core region but is outside the perimeter of the bound molecular orbitals of the ion core, the interaction between the photoelectron and the ion core can be viewed roughly as that between the photoelectron and the multipoles located at the center of mass of the ion. We call this region of the configuration space the *multipole-moment-interaction region*. When the photoelectron is inside the perimeter of the bound molecular orbitals, on the other hand, the interaction can no longer be viewed as that of the photoelectron and the multipole. Instead, the exchange interaction between the photoelectron and the bound electrons in the core dominates the motion of the photoelectron. This region of the configuration space is designated as the *electron-exchange-interaction region*.

In this paper, we present a theoretical formalism for the quantum-state-specific PADs from the direct photoionization of a diatomic molecule based on the quantum scattering theory formalism and angular momentum coupling algebra. Unlike the partial-wave formalism that was the basis of our previous work,<sup>11,27</sup> the present formalism treats explicitly the mixing between different  $l$  partial waves in the ion-core region, and it thus fully incorporates the molecular nature of the problem within the independent electron approximation. The resulting expressions clearly show the commonality between different photoionization processes and provide the relationship between the dipole-moment matrix elements that couples different ionizing states to the same ionization continuum. We note that most of the theoretical elements that form the basis of the present article have already appeared in the literature. The scattering theory formalism used in this article has been extensively developed to explain atomic Rydberg spectroscopy and photoionization by Seaton and co-workers<sup>28</sup> in the framework of the multichannel quantum defect theory (MQDT). MQDT has subsequently been adapted to molecular problems through the pioneering efforts of Fano, Jungen, Greene, and co-workers.<sup>23,24,26,29</sup> The angular momentum coupling expressions that appear in this article are, on the other hand, mostly adapted from our previous work<sup>11,27</sup> and that of McKoy and co-workers.<sup>30</sup> The present formalism is unique in its coupling of these two theoretical machineries that allows for a unified description of the direct photoionization of a molecule within the independent electron approximation.

Because many of the dynamical parameters that appear in this formalism pertain directly to the ionization continuum

without reference to the ionizing states, they should be common to photoionization processes from different ionizing states of a molecule as long as the same final state is reached, that is, as long as the rovibronic state of the ion and the energy of the photoelectron are the same. Emphasis is given to the clarification of basic physical ideas behind the theoretical formalism within the independent electron framework. The parallels between the ideas in this formalism and those used to describe atomic photoionization are also emphasized. The expressions given in this article can be used by an experimentalist to extract dynamical information on the molecular ionization continuum from the quantum-state-specific PADs; the procedure is illustrated in the companion article on the photoionization of NO.<sup>31</sup> This formalism can also be employed to predict experimental PADs based upon dynamical quantities obtained from theoretical calculations or from the spectroscopy of high-lying Rydberg states.

The organization of this article is as follows. In Sec. II, we outline the construction of the one-electron continuum molecular orbital for a photoelectron moving in the field of a diatomic-ion core. Section II begins with a brief discussion about the one-electron atomic continuum wave function to introduce the basic physical ideas and the machinery of scattering theory. In Sec. III, we present an expression for the quantum-state-specific PADs of a diatomic molecule based on the continuum-molecular-orbital decomposition developed in Sec. II. The spin part of various wave functions is not explicitly considered in Secs. II and III because we restrict ourselves to states of diatomic molecules that follow Hund's case (b) coupling. In Sec. IV, we discuss the applicability of the present formalism in retrieving information about the ionization continuum from experimental PADs. We also discuss briefly in Sec. IV the possible extension of the formalism to more general molecular photoionization problems. Appendix A contains a brief discussion about various matrices that appear in the main text; in Appendix B, we show the formal equivalence of the expressions in this article and those in the open-continuum MQDT.

## II. CONTINUUM MOLECULAR ORBITALS

Photoionization can be considered as an absorption of a photon followed by a half collision between the photoelectron and the ion. The final state reached by the photoabsorption is thus the collision state that describes the scattering event between the photoelectron and the ion. In this section, we construct the one-electron continuum wave function for a photoelectron moving in a diatomic-ion field based on the scattering theory formalism.<sup>29</sup> First, we briefly discuss the one-electron continuum wave function for a photoelectron moving in an atomic-ion field to lay the groundwork for the discussion of the molecular continuum wave functions. Because a photoelectron always moves under a central potential in the independent electron approximation in the case of atomic photoionization, the orbital angular momentum quantum number  $l$  for the photoelectron is a good quantum number. Consequently, the scattering between the photoelectron and the ion becomes a so-called "single-channel"

phenomenon,<sup>29</sup> and the discussion becomes particularly transparent. As will be seen, many of the quantities and ideas defined for the atomic continuum wave function can be directly carried over to the discussion of the molecular continuum wave function.

Because of the central nature of the ionic potential under which the photoelectron moves, the final state for the photoelectron in atomic photoionization can be expanded in partial waves<sup>29,32</sup> that conform to the incoming-wave boundary condition<sup>29</sup>

$$|\mathbf{k}'\rangle = \sum_{lm\lambda} i^l e^{-i\sigma_l} Y_{lm}^*(\hat{k}') \Psi_{lm}(\mathbf{r}'; k). \quad (1)$$

In Eq. (1),  $\mathbf{r}'$  is the position vector of the photoelectron in the laboratory (LAB) frame whose origin is located at the atomic nucleus, and  $\mathbf{k}' = k\hat{k}'$ , where  $\hat{k}'$  is the direction along which the photoelectron is ejected in the LAB frame. The quantity  $k$  is the magnitude of the asymptotic linear momentum of the photoelectron, which is related to the asymptotic photoelectron energy,  $\epsilon$ , by

$$\epsilon = \frac{k^2}{2m_e}, \quad (2)$$

where  $m_e$  designates the reduced mass of the electron. Atomic units are used throughout this article, and the meanings of angular momentum quantum numbers that appear in this article are listed in Table I.  $\sigma_l$  denotes the Coulomb phase shift, which is given by

$$\sigma_l \equiv \sigma_l(k) = \arg \Gamma(l+1 - im_e Z/k), \quad (3)$$

where  $Z$  is the net charge on the ion core. In photoionization of neutral species,  $Z=1$ , but we retain the symbol  $Z$  in the following expressions because many of the ideas developed in this section can be used to describe the ionization continuum for multiply charged ions as well. Although  $\sigma_l$  is an energy-dependent quantity, as is clear in Eq. (3) through its dependence on  $k$ , we do not explicitly indicate its energy dependence to make the notation more compact. In Eq. (1),  $\Psi_{lm}(\mathbf{r}'; k)$  is the energy-normalized wave function for the continuum electron referenced to the scattering amplitude  $S_l$ . The asymptotic form of  $\Psi_{lm}(\mathbf{r}'; k)$  is given by<sup>29,32</sup>

$$\Psi_{lm}(\mathbf{r}'; k) \xrightarrow{r \rightarrow \infty} \left( \frac{m_e}{\pi k} \right)^{1/2} \frac{1}{2ir} \times [e^{ix_l} - S_l^*(k) e^{-ix_l}] Y_{lm}(\hat{r}'), \quad (4)$$

where

$$x_l = kr - \frac{1}{2} l\pi - \frac{m_e Z}{k} \ln(2kr) + \sigma_l. \quad (5)$$

We also designate  $\Psi_{lm}(\mathbf{r}'; k)$  as the partial-wave basis function because it is the basis function that appears in the partial wave decomposition of the continuum state in Eq. (1). The coefficients on the right-hand side of Eq. (4) are chosen to ensure the normalization of  $\Psi_{lm}(\mathbf{r}'; k)$  per unit Rydberg energy interval. The scattering amplitude  $S_l$  designates the amplitude ratio of the outgoing and incoming wave components

TABLE I. Angular momentum quantum numbers used in the text.

Angular momentum	Laboratory fixed projection	Molecule-fixed projection	Description
$N$	$M_N$	$\Lambda$	Nuclear rotation plus orbital angular momentum for the ionizing state
$N^+$	$M^+$	$\Lambda^+$	Nuclear rotation plus orbital angular momentum for the ion
$N_i$	$M_i$	$\Lambda_i$	Angular momentum transferred between the photoelectron and the ion
$J$	$M_J$	$\Lambda_J$	Total angular momentum (excluding nuclear and electronic spins)
$l$	$m$	$\lambda$	Photoelectron angular momentum
1	$\mu_0$	$\mu$	Photon angular momentum

for each value of  $l$ ,<sup>29</sup> and it can be related to the scattering phase shift,  $\rho_l \equiv \rho_l(k)$  (modulo  $\pi$ ), by the relation

$$S_l(k) = e^{2i\pi\rho_l}. \quad (6)$$

The physical meaning of  $\rho_l$  will be discussed below.

Because the photoelectron moves under the Coulombic potential in the asymptotic region, the one-electron continuum wave function in that region can be *exactly* represented as a linear combination of the regular and irregular Coulomb basis functions,  $f_l$  and  $g_l$ , respectively. Here,  $f_l$  and  $g_l$  are two linearly independent solutions of the radial Schrödinger equation for the Coulombic potential whose analytical properties are well documented<sup>28</sup> and whose asymptotic forms are given by<sup>24</sup>

$$f_l(r;k) \xrightarrow{r \rightarrow \infty} \left(\frac{2m_e}{\pi k}\right)^{1/2} \sin x_l$$

and

$$g_l(r;k) \xrightarrow{r \rightarrow \infty} -\left(\frac{2m_e}{\pi k}\right)^{1/2} \cos x_l. \quad (7)$$

We thus introduce a continuum wave function that is the linear combination of  $f_l$  and  $g_l$  in the asymptotic region

$$\Phi_{lm}(\mathbf{r}';k) = \frac{1}{\sqrt{2r}} [f_l(r;k) - K_l(k)g_l(r;k)] Y_{lm}(\hat{r}') \quad (r > r_0). \quad (8)$$

Here,  $r_0$  designates a radial distance from the atomic nucleus to a (fictitious) surface that divides the ion-core region and the asymptotic region. In Eq. (8),  $K_l$  is called the *reaction amplitude* and is given by

$$K_l(k) = \tan(\pi\rho_l). \quad (9)$$

The reaction amplitude  $K_l$  represents the ratio of  $g_l$  with respect to  $f_l$  in  $\Phi_{lm}(\mathbf{r}';k)$ . Note that the radial part of  $\Phi_{lm}(\mathbf{r}';k)$  is real, whereas that of  $\Psi_{lm}(\mathbf{r}';k)$  is complex. The fact that  $g_l$  appears in  $\Phi_{lm}(\mathbf{r}';k)$  is a direct manifestation of the presence of other electrons in the ion-core region.<sup>33</sup>

When the ion is hydrogenic, that is, when there are no other electrons except the electron being ionized in the ion-core region, the potential under which the photoelectron moves is always Coulombic. In this case, the irregular Coulomb basis function,  $g_l$ , cannot be a part of the acceptable continuum wave function because of the boundary condition at the origin. When there are other electrons, however,  $g_l$  can be a part of  $\Phi_{lm}(\mathbf{r}';k)$  outside the ion-core region because the boundary condition at the origin is lifted; the ion-core region is effectively treated as a “black box,” and the boundary is moved to  $r=r_0$ . The complex interaction between the photoelectron and the other electrons in the ion-core region is nevertheless wholly represented by the scattering phase shift  $\rho_l$  (or equivalently the scattering amplitude  $S_l$  and the reaction amplitude  $K_l$ ) outside the ion-core region.<sup>29</sup> The relationship between  $\Phi_{lm}(\mathbf{r}';k)$  and  $\Psi_{lm}(\mathbf{r}';k)$  is given by

$$\Psi_{lm}(\mathbf{r}';k) = [1 + iK_l(k)]^{-1} \Phi_{lm}(\mathbf{r}';k), \quad (10)$$

as can be shown easily from Eqs. (4) through (8). We note that  $\Phi_{lm}(\mathbf{r}';k)$  is not normalized per unit Rydberg energy interval and thus introduce another one-electron wave function  $\Xi_{lm}(\mathbf{r}';k)$  that is properly normalized:

$$\Xi_{lm}(\mathbf{r}';k) = \cos(\pi\rho_l) \Phi_{lm}(\mathbf{r}';k). \quad (11)$$

By substituting Eqs. (9) to (11) into Eq. (1), we obtain the photoelectron final-state wave function  $|\mathbf{k}'\rangle$  expressed in terms of  $\Xi_{lm}(\mathbf{r}';k)$ .

Before we proceed to a discussion of the final one-electron state for the molecular photoionization, a comment on the physical meanings of quantities that have been introduced so far is appropriate. The scattering phase shift  $\rho_l$  carries information on how the ion-core short-range interaction affects each partial-wave channel in the asymptotic region. It is also an analytic continuation of the quantum defect defined for the Rydberg states of the atom.<sup>28</sup> Because the photoelectron moves in the deep Coulomb well near the ion core with a large associated kinetic energy, the dynamics inside the ion-core region and thus  $\rho_l$  are not very sensitive to the asymptotic photoelectron energy.<sup>34</sup> The sensitivity of  $\rho_l$  to the

photoelectron energy is roughly proportional to the ratio of the energy variation to the ionization potential of the atom. When the variation of the asymptotic photoelectron energy is small,  $\rho_l$  can therefore be approximated to be independent of energy and can be compared with the quantum defect for the high-lying Rydberg states of the atom. The complicated energy dependence of the one-electron continuum wave functions  $\Phi_{lm}(\mathbf{r}';k)$  and  $\Xi_{lm}(\mathbf{r}';k)$  that stems from the electronic motion in the asymptotic region is compactly represented by the well-known properties of the regular and irregular Coulomb basis functions  $f_l$  and  $g_l$  and the Coulomb phase shift  $\sigma_l$ .<sup>24,29</sup>

The wave function  $\Xi_{lm}(\mathbf{r}';k)$  [and  $\Psi_{lm}(\mathbf{r}';k)$ ] is the one-electron eigenfunction of both the orbital angular momentum operator and the atomic Hamiltonian. Therefore, it can be identified as the *continuum atomic orbital*, setting aside the asymptotic boundary condition that should be applied to it through Eqs. (1) and (11). Several differences exist, however, between  $\Xi_{lm}(\mathbf{r}';k)$  and bound atomic orbitals that are commonly encountered in electronic structure calculations. Whereas a bound atomic orbital is defined only at a specific orbital energy,  $\Xi_{lm}(\mathbf{r}';k)$  is defined at every energy  $\epsilon$ . For a given photoelectron energy  $\epsilon$ , an infinite number of  $\Xi_{lm}(\mathbf{r}';k)$  exist that are degenerate. Being a continuum wave function,  $\Xi_{lm}(\mathbf{r}';k)$  is normalized to the Dirac delta function, that is,  $\Xi_{lm}(\mathbf{r}';k)$  is an improper vector in the physical Hilbert space.<sup>35</sup> For this reason, we cannot interpret  $\Xi_{lm}^*(\mathbf{r}';k)\Xi_{lm}(\mathbf{r}';k)$  as representing the probability density of finding a photoelectron at a specific point in the configuration space, unlike the case for bound orbitals. These differences are manifestations of the fact that  $\Xi_{lm}(\mathbf{r}';k)$  is defined for the continuum electron ( $\epsilon > 0$ ).

The expressions for the final state in molecular photoionization can be obtained following a similar procedure. The fact that the molecular ion has a structure associated with it, however, introduces two important modifications in the resulting expressions. First, any one-electron wave function for the molecular ionization continuum should be referenced to the molecule-fixed (MF) frame. Second, the potential under which the photoelectron moves in the ion-core region is noncentral, and the scattering between the photoelectron and the ion core becomes a ‘‘multichannel’’ problem.<sup>29</sup> The photoelectron motion in the asymptotic region is nevertheless governed by the Coulombic potential as discussed in Sec. I, and the one-electron final-state wave function for the photoelectron in the photoionization of a diatomic molecule can be expanded in partial waves<sup>30,36</sup> that conform to the incoming-wave boundary condition,<sup>37</sup> just as for the one-electron final-state wave function for the photoelectron in the atomic photoionization

$$|\mathbf{k}';R\rangle = \sum_{lm} i^l e^{-i\sigma_l} Y_{lm}^*(\hat{k}') D_{m\lambda}^{l*}(\hat{R}) \psi_{l\lambda}(\mathbf{r};k,R). \quad (12)$$

Here,  $\mathbf{k}'$  and  $\sigma_l$  are defined in the same way as in the atomic photoionization [see Eqs. (2) and (3)], and  $R$  is the internuclear distance of the molecular ion. In Eq. (12),  $\mathbf{r}$  designates the position vector of the photoelectron in the molecule-fixed

(MF) frame. The coordinate systems are defined such that the  $z$  axis of the MF frame is along the internuclear axis of the molecular ion and the origin of the MF frame coincides with that of the LAB frame at the center of mass (CM) of the ion. Thus the two frames are related to each other through a frame rotation by a set of three Euler angles  $\hat{R}$ . Whenever there is no ambiguity, we adopt a convention that a vector with a prime is expressed in the LAB frame, whereas a vector without a prime is expressed in the MF frame. Comparison of Eqs. (1) and (12) shows that the rotation matrix element  $D_{m\lambda}^{l*}(\hat{R})$  appears in Eq. (12) because the one-electron wave function  $\psi_{l\lambda}(\mathbf{r};k,R)$  is expressed in the MF frame. Here,  $\psi_{l\lambda}(\mathbf{r};k,R)$  is the energy-normalized one-electron wave function for the continuum electron referenced to the MF-frame scattering matrix (**S** matrix). The asymptotic form of  $\psi_{l\lambda}(\mathbf{r};k,R)$  is given by<sup>38</sup>

$$\psi_{l\lambda}(\mathbf{r};k,R) \xrightarrow{r \rightarrow \infty} \left(\frac{m_e}{\pi k}\right)^{1/2} \frac{1}{2ir} \times \sum_{l' \geq |\lambda|} [e^{ix_{l'}} \delta_{ll'} - S_{ll'}^{\lambda*}(k,R) e^{-ix_{l'}}] Y_{l'\lambda}(\hat{r}). \quad (13)$$

The molecular wave function  $\psi_{l\lambda}(\mathbf{r};k,R)$  is also designated as the partial-wave basis function, just as  $\Psi_{lm}(\mathbf{r}';k)$  is in atomic photoionization.  $S_{ll'}^{\lambda}$  is the  $(l, l')$  element of the **S** matrix for a given value of  $\lambda$ , which is the  $z$ -axis projection of  $l$  in the MF frame. The **S** matrix is the multichannel analog of the scattering amplitude,  $S_l$ , defined in Eq. (4). Together with the incoming-wave boundary condition presented in Eq. (12), the form of Eq. (13) ensures that for large  $r$  the continuum wave function is composed of one outgoing Coulomb wave with  $l$  and the incoming Coulomb waves with all  $l'$ , consistent with the time-dependent representation of the photoionization process.<sup>37,39</sup>

Inspection of  $\psi_{l\lambda}(\mathbf{r};k,R)$  in Eq. (13) clearly reveals the molecular nature of the continuum wave function despite its asymptotic form. Although the photoelectron experiences the spherical Coulombic potential when it is in the asymptotic region, it moves under the nonspherical molecular potential when it is inside the ion-core region. Thus  $l$  is not a good quantum number in this region, and the  $l$ -mixing between different partial waves, or equivalently the  $l$ -changing collision between the photoelectron and the ion core, can occur when the photoelectron emerges from the ion core. In the independent electron approximation, however,  $\lambda$  is still a good quantum number because of the cylindrical nature of the diatomic-ion-core potential. The possibility of  $l$ -changing collisions within the same  $\lambda$  manifold is indicated in Eq. (13) by off-diagonal elements of the **S** <sup>$\lambda$</sup>  matrix,  $S_{ll'}^{\lambda}$  ( $l \neq l'$ ). The **S** <sup>$\lambda$</sup>  matrix designates a portion of the full **S** matrix that is block diagonal in  $\lambda$ .  $S_{ll'}^{\lambda}$  gives the amplitude ratio of the outgoing Coulomb wave with  $l$  and incoming Coulomb wave with  $l'$  for each value of  $\lambda$ . It is important to note that  $S_{ll'}^{\lambda}$ , being a continuum property, is a function of the asymptotic energy of the photoelectron and the internuclear distance only. The **S** <sup>$\lambda$</sup>  matrix is a unitary matrix, and it com-

TABLE II. Glossary of terms used in the text.

Term		Description <sup>a</sup>
Atomic case (Spherical potential)	Diatomic (Cylindrical potential)	
$\sigma_l(k)$	$\sigma_l(k)$	Coulomb phase shift
$l$	$\alpha_\lambda$	Electronic eigenchannel index; Orbital index
$S_l(k)\delta_{ll'}$	$S_{ll'}^\lambda(k,R)$	$(l,l')$ element of the scattering matrix (for a given value of $\lambda$ )
$K_l(k)\delta_{ll'}$	$K_{ll'}^\lambda(k,R)$	$(l,l')$ element of the reaction matrix (for a given value of $\lambda$ )
$\delta_{ll'}$	$U_{l\alpha_\lambda}^\lambda(k,R)$	$(l,l')$ element of the electronic transformation matrix ( $(l,\alpha_\lambda)$ element for a given value of $\lambda$ )
$\rho_l(k)$	$\tau_{\alpha_\lambda}^\lambda$	Electronic eigenphase shift
$ \mathbf{k}'\rangle$	$ \mathbf{k}';R\rangle$	Photoelectron final-state wave function
$\Psi_{lm}(\mathbf{r}';k)$	$\psi_{l\lambda}(\mathbf{r};k,R)$	Continuum one-electron wave function referenced to the scattering matrix; Partial-wave basis function
$\Phi_{lm}(\mathbf{r}';k)$	$\varphi_{l\lambda}(\mathbf{r};k,R)$	Continuum one-electron wave function referenced to the reaction matrix
$\Xi_{lm}(\mathbf{r}';k)$	$\xi_{\alpha_\lambda}^\lambda(\mathbf{r};k,R)$	Electronic eigenchannel wave function; Continuum orbital

<sup>a</sup>The descriptions in parentheses apply only to diatomic molecules.

pletely specifies the asymptotic outcome of the collision between the photoelectron and the ion core for a given  $\lambda$ .

For the same reason as for the atomic continuum wave function, the one-electron continuum wave function for the molecule can be expressed as a linear combination of  $f_l$  and  $g_l$  in the asymptotic region. We thus introduce the continuum wave function that is referenced to the MF-frame reaction matrix ( $\mathbf{K}$  matrix),<sup>38</sup>  $\varphi_{l\lambda}(\mathbf{r};k,R)$ , which is the multichannel analog of  $\Phi_{lm}(\mathbf{r}';k)$  for an atom

$$\begin{aligned} \varphi_{l\lambda}(\mathbf{r};k,R) = & \frac{1}{\sqrt{2}r} \sum_{l' \geq |\lambda|} [f_{l'}(r;k)\delta_{ll'} \\ & - K_{ll'}^\lambda(k,R)g_{l'}(r;k)]Y_{l'\lambda}(\hat{r}) \quad (r > r_0). \end{aligned} \quad (14)$$

Once again,  $r_0$  is a radial distance from the CM of the ion core to a (fictitious) surface that divides the ion-core region and the asymptotic region,  $\mathbf{I}$  is the unit matrix, and  $\mathbf{K}^\lambda$  is the MF-frame reaction matrix for a given  $\lambda$ . The  $\mathbf{K}$  matrix is the multichannel analog of the reaction amplitude  $K_l$  that appears in Eq. (8). The full  $\mathbf{K}$  matrix is block diagonal in  $\lambda$  for the same reason the  $\mathbf{S}$  matrix is. The matrix element  $K_{ll'}^\lambda$  signifies the ratio of  $g_{l'}$  with respect to  $f_l$  in  $\varphi_{l\lambda}(\mathbf{r};k,R)$ , and it is a function of the photoelectron energy and internuclear distance only, just as  $S_{ll'}^\lambda$  is. The relation between the  $\mathbf{S}$  matrix and the  $\mathbf{K}$  matrix is given by<sup>40</sup>

$$\sum_{l'} S_{ll'}^\lambda (\delta_{l'l''} - iK_{l'l''}^\lambda) = \delta_{ll''} + iK_{ll''}^\lambda, \quad (15a)$$

which can be rewritten in matrix notation as

$$\mathbf{S}^\lambda = \frac{\mathbf{I} + i\mathbf{K}^\lambda}{\mathbf{I} - i\mathbf{K}^\lambda}. \quad (15b)$$

Whereas the  $\mathbf{S}^\lambda$  matrix is a complex unitary matrix, the  $\mathbf{K}^\lambda$  matrix is a real symmetric matrix (a real Hermitian matrix). Thus  $\varphi_{l\lambda}(\mathbf{r};k,R)$  has a real radial part whereas the radial part of  $\psi_{l\lambda}(\mathbf{r};k,R)$  is complex. Using Eqs. (13) through (15), it can be shown that  $\psi_{l\lambda}(\mathbf{r};k,R)$  and  $\varphi_{l\lambda}(\mathbf{r};k,R)$  are related to each other by the following equality:<sup>38,41</sup>

$$\psi_{l\lambda}(\mathbf{r};k,R) = \sum_{l' \geq |\lambda|} [\mathbf{I} + i\mathbf{K}^\lambda]_{ll'}^{-1} \varphi_{l'\lambda}(\mathbf{r};k,R). \quad (16)$$

Just as  $S_l$  and  $K_l$  defined for an atom do, both the  $\mathbf{S}^\lambda$  and  $\mathbf{K}^\lambda$  matrices completely specify the asymptotic outcome of the electron scattering from the (linear) molecular ion core for a given  $\lambda$ . The effect of the complex interactions that the photoelectron experiences inside the ion-core region is thus wholly represented by the  $\mathbf{K}$  matrix outside the ion-core region. We emphasize that the  $\mathbf{K}^\lambda$  matrix defined in Eqs. (14) and (15), like  $K_l$  that appears in the atomic continuum wave function, characterizes only the short-range collision dynamics between the photoelectron and the ion core because of the anisotropic molecular-ion-core potential.<sup>24,28</sup> Because the electron moves in the deep Coulomb well near the ion core, the short-range dynamics and thus the  $\mathbf{K}$  matrix are rather insensitive to the asymptotic photoelectron energy, just as  $K_l$  is insensitive. In many applications, the  $\mathbf{K}$  matrix can be treated to be approximately independent of energy.

To this point, the discussion reveals the nearly one-to-one correspondence between various quantities defined for molecular and atomic photoelectrons;  $\mathbf{S}^\lambda$ ,  $\mathbf{K}^\lambda$ ,  $\psi_{l\lambda}(\mathbf{r};k,R)$ , and  $\varphi_{l\lambda}(\mathbf{r};k,R)$  are the multichannel analogs of  $S_l$ ,  $K_l$ ,  $\Psi_{lm}(\mathbf{r}';k)$ , and  $\Phi_{lm}(\mathbf{r}';k)$ , respectively. This correspondence becomes more evident when we consider the scattering amplitude  $S_l$  and the reaction amplitude  $K_l$  defined for the atomic photoelectron as the diagonal elements of the scatter-

ing matrix and the reaction matrix, respectively (see Table II). Because of the central nature of the atomic potential, the off-diagonal elements of these matrices are all zero in the atomic case. Note, however, that the one-electron wave functions  $\psi_{l\lambda}(\mathbf{r};k,R)$  and  $\varphi_{l\lambda}(\mathbf{r};k,R)$  defined for the molecular photoelectron are not the eigenfunctions of the molecular Hamiltonian in the ion-core region, as can be seen from the off-diagonal elements of the  $\mathbf{S}^\lambda$  and  $\mathbf{K}^\lambda$  matrices. The atomic counterparts of them,  $\Psi_{lm}(\mathbf{r}';k)$  and  $\Phi_{lm}(\mathbf{r}';k)$ , are eigenfunctions of the atomic Hamiltonian throughout the configuration space for the photoelectron in the independent electron approximation. Indeed  $\psi_{l\lambda}(\mathbf{r};k,R)$  and  $\varphi_{l\lambda}(\mathbf{r};k,R)$  can be rewritten in terms of another set of one-electron wave functions that are eigenfunctions of the short-range molecular Hamiltonian based on the eigenchannel formulation of scattering theory.<sup>23,24,42,43</sup> The derivation is briefly outlined below.

Because the  $\mathbf{K}^\lambda$  matrix is real and symmetric, it can be diagonalized by the unitary transformation

$$\begin{aligned} K_{ll'}^\lambda &= \sum_{\alpha_\lambda} U_{l\alpha_\lambda}^\lambda (\tan \pi\tau_{\alpha_\lambda}^\lambda) U_{\alpha_\lambda l'}^{\lambda T} \\ &= \sum_{\alpha_\lambda} U_{l\alpha_\lambda}^\lambda (\tan \pi\tau_{\alpha_\lambda}^\lambda) U_{l'\alpha_\lambda}^\lambda. \end{aligned} \quad (17a)$$

Equation (17a) can be written in the matrix form

$$\mathbf{K}^\lambda = \mathbf{U}^\lambda (\mathbf{\tan} \pi\tau^\lambda) (\mathbf{U}^\lambda)^T, \quad (17b)$$

where  $\mathbf{U}^\lambda$  is an *electronic transformation matrix* that diagonalizes the  $\mathbf{K}^\lambda$  matrix,  $(\mathbf{U}^\lambda)^T$  is the transpose of  $\mathbf{U}^\lambda$ , and  $\mathbf{\tan} \pi\tau^\lambda$  is a diagonal matrix with the element  $\tan \pi\tau_{\alpha_\lambda}^\lambda$  on the  $\alpha_\lambda$ th row. Because  $\mathbf{K}^\lambda$  is a real matrix, we may choose  $\mathbf{U}^\lambda$  to be a real orthogonal matrix. We designate  $\alpha_\lambda$  as the *electronic eigenchannel index* or the *molecular orbital index* and  $\tau_{\alpha_\lambda}^\lambda$  as the *electronic eigenphase shift*.

Using Eq. (17) and the real unitary property of  $\mathbf{U}^\lambda$ , it can be easily shown that

$$[\mathbf{I} + i\mathbf{K}^\lambda]^{-1} = \mathbf{U}^\lambda (\mathbf{e}^{-i\pi\tau^\lambda} \mathbf{\cos} \pi\tau^\lambda) (\mathbf{U}^\lambda)^T. \quad (18)$$

Here,  $\mathbf{e}^{-i\pi\tau^\lambda} \mathbf{\cos} \pi\tau^\lambda$  is a diagonal matrix with  $e^{-i\pi\tau_{\alpha_\lambda}^\lambda} \cos \pi\tau_{\alpha_\lambda}^\lambda$  on the  $\alpha_\lambda$ th row. Equation (18) can be inserted into Eq. (16) to obtain

$$\begin{aligned} \psi_{l\lambda}(\mathbf{r};k,R) &= \sum_{l'} \sum_{\alpha_\lambda} U_{l\alpha_\lambda}^\lambda e^{-i\pi\tau_{\alpha_\lambda}^\lambda} (\cos \pi\tau_{\alpha_\lambda}^\lambda) \\ &\quad \times U_{l'\alpha_\lambda}^\lambda \varphi_{l'\lambda}(\mathbf{r};k,R). \end{aligned} \quad (19)$$

Using Eq. (14) and the normalization properties of  $\mathbf{U}^\lambda$ ,

$$\sum_l U_{l\alpha_\lambda}^\lambda U_{l\alpha'_\lambda}^\lambda = \delta_{\alpha_\lambda\alpha'_\lambda}, \quad \sum_{\alpha_\lambda} U_{l\alpha_\lambda}^\lambda U_{l'\alpha_\lambda}^\lambda = \delta_{ll'}, \quad (20)$$

we can rewrite Eq. (19) as

$$\psi_{l\lambda}(\mathbf{r};k,R) = \sum_{\alpha_\lambda} U_{l\alpha_\lambda}^\lambda e^{-i\pi\tau_{\alpha_\lambda}^\lambda} \xi_{\alpha_\lambda}^\lambda(\mathbf{r};k,R), \quad (21)$$

where  $\xi_{\alpha_\lambda}^\lambda(\mathbf{r};k,R)$  is given by

$$\begin{aligned} \xi_{\alpha_\lambda}^\lambda(\mathbf{r};k,R) &= \frac{1}{\sqrt{2r}} \sum_{l''} U_{l''\alpha_\lambda}^\lambda [f_{l''}(r;k) (\cos \pi\tau_{\alpha_\lambda}^\lambda) \\ &\quad - g_{l''}(r;k) (\sin \pi\tau_{\alpha_\lambda}^\lambda)] Y_{l''\lambda}(\hat{r}) \quad (r > r_0). \end{aligned} \quad (22)$$

The wave function  $\xi_{\alpha_\lambda}^\lambda(\mathbf{r};k,R)$  is designated as the *electronic eigenchannel wave function*.<sup>24,43</sup> Finally, by inserting Eq. (21) into Eq. (11), we can write the one-electron continuum state that conforms to the incoming-wave boundary condition as

$$\begin{aligned} |\mathbf{k}';R\rangle &= \sum_{lm\lambda} i^l e^{-i\sigma_l} Y_{lm}^*(\hat{k}') D_{m\lambda}^{l*}(\hat{R}) \\ &\quad \times \sum_{\alpha_\lambda} U_{l\alpha_\lambda}^\lambda e^{-i\pi\tau_{\alpha_\lambda}^\lambda} \xi_{\alpha_\lambda}^\lambda(\mathbf{r};k,R). \end{aligned} \quad (23)$$

Before we proceed to the next section, we should investigate the physical meanings of  $\tau_{\alpha_\lambda}^\lambda$ ,  $U_{l\alpha_\lambda}^\lambda$ , and  $\xi_{\alpha_\lambda}^\lambda(\mathbf{r};k,R)$ , which were designated as the electronic eigenphase shift, the electronic transformation matrix element, and the electronic eigenchannel wave function, respectively.  $\xi_{\alpha_\lambda}^\lambda(\mathbf{r};k,R)$  defined in Eq. (22) is an admixture of  $f_l$  and  $g_l$  with various  $l$  just like  $\varphi_{l\lambda}(\mathbf{r};k,R)$  in Eq. (14). Mathematically, the  $\xi_{\alpha_\lambda}^\lambda(\mathbf{r};k,R)$  and the  $\varphi_{l\lambda}(\mathbf{r};k,R)$  are independent basis sets that are related to each other by the orthogonal transformation matrix  $\mathbf{U}^\lambda$  (aside from the factor  $\cos \pi\tau_{\alpha_\lambda}^\lambda$ ). The  $f_l$  and  $g_l$  that appear in  $\xi_{\alpha_\lambda}^\lambda(\mathbf{r};k,R)$  are, however, weighted regardless of  $l$  with the same quantities,  $\cos \pi\tau_{\alpha_\lambda}^\lambda$  and  $\sin \pi\tau_{\alpha_\lambda}^\lambda$ , respectively, unlike those in  $\varphi_{l\lambda}(\mathbf{r};k,R)$ . This observation indicates that  $\xi_{\alpha_\lambda}^\lambda(\mathbf{r};k,R)$  is an eigenbasis that diagonalizes the  $\mathbf{K}^\lambda$  matrix.<sup>24,43</sup> Because the  $\mathbf{K}^\lambda$  matrix characterizes the scattering process between the photoelectron and the ion core for a given  $\lambda$ ,  $\xi_{\alpha_\lambda}^\lambda(\mathbf{r};k,R)$  is the eigenfunction of the collision process described by the  $\mathbf{K}^\lambda$  matrix. In addition, because  $\xi_{\alpha_\lambda}^\lambda(\mathbf{r};k,R)$  and  $\xi_{\alpha'_\lambda}^\lambda(\mathbf{r};k,R)$  ( $\alpha_\lambda \neq \alpha'_\lambda$ ) are not mixed by the scattering of the electron from the ion core, there should be no short-range interaction that couples  $\xi_{\alpha_\lambda}^\lambda(\mathbf{r};k,R)$  and  $\xi_{\alpha'_\lambda}^\lambda(\mathbf{r};k,R)$ .<sup>24</sup> This lack of short-range mixing means that  $\xi_{\alpha_\lambda}^\lambda(\mathbf{r};k,R)$  is also an eigenfunction of the short-range MF-frame electronic Hamiltonian at a given asymptotic energy of the photoelectron and the internuclear distance  $R$ .

Quantum mechanically, any linear combination of various Coulomb basis functions,  $f_l$  and  $g_l$ , with the same  $k$  and  $R$  can be considered an eigenfunction of the MF-frame electronic Hamiltonian as long as it conforms to the appropriate boundary conditions because all of the linear combinations are defined to be degenerate. They are related to each other by an appropriate unitary transformation. Among these eigenfunctions, however, the partial-wave basis function  $\psi_{l\lambda}(\mathbf{r};k,R)$  and the electronic eigenchannel wave function  $\xi_{\alpha_\lambda}^\lambda(\mathbf{r};k,R)$  stand out because of their physical significance.  $\psi_{l\lambda}(\mathbf{r};k,R)$  is the basis function for the partial-wave decom-

position of the continuum wave function,  $|\mathbf{k}';R\rangle$ . Because asymptotically it is composed of the incoming and outgoing Coulomb waves, the physical boundary condition at infinity that is appropriate for the photoionization process can be easily applied to  $\psi_{l\lambda}(\mathbf{r};k,R)$ . On the other hand,  $\xi_{\alpha\lambda}^{\lambda}(\mathbf{r};k,R)$  is the eigenbasis for the collision between the photoelectron and the molecular-ion core that is described by the electronic  $\mathbf{K}^{\lambda}$  matrix.<sup>24,43</sup> It is also the one-electron eigenfunction of the short-range electronic Hamiltonian at a fixed nuclear geometry.

Considering that the short-range Hamiltonian is what characterizes the molecular nature of the scattering process,  $\xi_{\alpha\lambda}^{\lambda}(\mathbf{r};k,R)$  can be appropriately designated as the *continuum molecular orbital*. Just like the continuum atomic orbital, the continuum molecular orbitals have the following properties:  $\xi_{\alpha\lambda}^{\lambda}(\mathbf{r};k,R)$  is defined at every energy,  $\epsilon$ . For a given photoelectron energy  $\epsilon$ , there are infinite number of  $\xi_{\alpha\lambda}^{\lambda}(\mathbf{r};k,R)$  that are degenerate. Because  $\xi_{\alpha\lambda}^{\lambda}(\mathbf{r};k,R)$  is an improper vector in the physical Hilbert space, we cannot interpret  $\xi_{\alpha\lambda}^{\lambda*}(\mathbf{r};k,R)\xi_{\alpha\lambda}^{\lambda}(\mathbf{r};k,R)$  as representing the probability density of finding the electron at a specific point of the configuration space.

With the above interpretations of  $\xi_{\alpha\lambda}^{\lambda}(\mathbf{r};k,R)$  in mind, it is straightforward to assess the physical meanings of  $\tau_{\alpha\lambda}^{\lambda}$  and  $U_{l\alpha\lambda}^{\lambda}$ . The electronic eigenphase-shift  $\tau_{\alpha\lambda}^{\lambda}$  is a scattering phase shift associated with the electronic eigenchannel wave function  $\xi_{\alpha\lambda}^{\lambda}(\mathbf{r};k,R)$  at a given  $k$  and  $R$ . It carries information about how the ion-core short-range potential acts on each electronic eigenchannel.  $\tau_{\alpha\lambda}^{\lambda}$  is also an analytic continuation of the electronic quantum defect defined for the Rydberg states of molecules.<sup>28</sup> Because of the insensitivity of the short-range scattering dynamics to the energy of the photoelectron,  $\tau_{\alpha\lambda}^{\lambda}$  can be compared with the corresponding electronic quantum defect of high-lying Rydberg states obtained from MQDT analysis of Rydberg spectra.<sup>44</sup> The correspondence between  $\tau_{\alpha\lambda}^{\lambda}$  defined for molecules and  $\rho_l$  defined for atoms can be recognized immediately (see Table II).  $U_{l\alpha\lambda}^{\lambda}$ , which is defined to be the element of the electronic transformation matrix that diagonalizes the  $\mathbf{K}^{\lambda}$  matrix, can be interpreted as the projection of a partial-wave wave function onto the eigenstate of the collision (or of the short-range Hamiltonian) for a given  $k$  and  $R$ . As for  $\tau_{\alpha\lambda}^{\lambda}$ ,  $U_{l\alpha\lambda}^{\lambda}$  can be compared with the Rydberg-series mixing coefficient that can be determined from the spectroscopy of Rydberg states.<sup>44</sup>

### III. DIPOLE-MOMENT MATRIX ELEMENTS AND PHOTOELECTRON ANGULAR DISTRIBUTIONS

The dynamics of one-photon ionization in the weak-field limit is governed by the electric dipole-moment matrix elements that connect the ionizing state to the ionization continuum. Thus an expression for the quantum-state-specific PADs can be obtained from expressions for these dipole matrix elements. In this section, we derive an expression for the PAD when both the ionizing state and the state of the ion are

described by Hund's case (b) coupling. The derivation given in this article can be easily extended to other Hund's coupling cases. The approximations made in the derivation are also discussed in detail in this section. We note that the same approximations were used in the earlier literature on this subject without explicit justification.<sup>11,27</sup>

The wave function for an ionizing state that follows Hund's case (b) coupling is given by the Born–Oppenheimer product

$$|\Psi_{p\nu N\Lambda M_N}\rangle = \left(\frac{2N+1}{8\pi^2}\right)^{1/2} |p\Lambda\rangle \chi_{\nu}(R) D_{M_N\Lambda}^{N*}(\hat{R}). \quad (24)$$

Here,  $\nu$  is the vibrational quantum number for the ionizing state, and  $p$  represents quantum numbers needed to specify the ionizing state completely. All the angular momentum quantum numbers are listed in Table I.  $\chi_{\nu}(R)$  is a vibrational wave function in the ionizing state that we set to be real. The wave function for the composite state of the photoelectron and the ion that follows Hund's case (b) coupling can also be written as a similar Born–Oppenheimer type product using the one-electron continuum wave functions given in Eq. (12)

$$\begin{aligned} |\Psi_{p^+\nu^+ N^+ \Lambda^+ M^+; \mathbf{k}'\rangle &= \left(\frac{2N^++1}{8\pi^2}\right)^{1/2} \chi_{\nu^+}(R) D_{M^+ \Lambda^+}^{N^+*}(\hat{R}) \\ &\times \sum_{lm\lambda} i^l e^{-i\sigma_l} Y_{lm}^*(\hat{k}') D_{m\lambda}^{l*}(\hat{R}) \\ &\times \tilde{\mathbf{A}}[|\psi_{l\lambda}(\mathbf{r};k,R)\rangle |p^+ \Lambda^+\rangle]. \end{aligned} \quad (25)$$

Here,  $\nu^+$  represents the vibrational quantum number for the ion,  $p^+$  represents the quantum numbers needed to specify the state of the ion completely, and  $\chi_{\nu^+}(R)$  represents a vibrational wave function in the ion electronic state.  $\tilde{\mathbf{A}}$  designates the antisymmetrization operator.

Several approximations are implicit in writing the wave functions as in Eqs. (24) and (25). The spin parts of both wave functions are not explicitly written because the spins are decoupled from the dynamics when we assume Hund's case (b) coupling. This choice is equivalent to assuming that the spins remain coupled throughout the ionization process to the spin value of the ionizing state.<sup>24</sup> The wave functions given for both the ionizing state and the final state are also not parity adapted. Because we do not consider the interactions that remove the degeneracy between different parity states, the final results of our derivation remain the same when we use parity adapted wave functions, provided that the incoherent sum over each parity component is performed at the appropriate stage. Finally, by writing the final-state wave function as Born–Oppenheimer products as in Eq. (25), we are ignoring the coupling between nuclear vibrational motion and the electron being ionized when it is near the ion core. When the photoelectron is inside the ion-core region, the vibrational wave function for the composite state of the photoelectron and the ion can be slightly different from that of the isolated ion.<sup>26</sup>

The transition electric-dipole-moment matrix element that connects the ionizing state and the final state in our formalism is given by



$$\begin{aligned}
& \langle \Psi_{p^+ \nu^+ N^+ \Lambda^+ M^+; \mathbf{k}'} | D_{\mu_0} | \Psi_{p \nu N \Lambda M_N} \rangle \\
& \equiv \left\langle \Psi_{p^+ \nu^+ N^+ \Lambda^+ M^+; \mathbf{k}'} \left| \sum_s \mathbf{r}'_s \cdot \hat{\boldsymbol{\epsilon}}' \right| \Psi_{p \nu N \Lambda M_N} \right\rangle \\
& = \left( \frac{4\pi}{3} \right)^{1/2} \left\langle \Psi_{p^+ \nu^+ N^+ \Lambda^+ M^+; \mathbf{k}'} \left| \sum_s r_s Y_{1\mu_0}(\hat{r}'_s) \right. \right. \\
& \quad \left. \left. \times \left| \Psi_{p \nu N \Lambda M_N} \right. \right. \right\rangle, \quad (26)
\end{aligned}$$

where  $\mathbf{r}'_s$  is the electronic coordinate expressed in the LAB frame,  $\hat{\boldsymbol{\epsilon}}'$  is the unit polarization vector of light in the LAB

frame, and  $s$  is an index that runs over all electrons in the molecule.  $D_{\mu_0}$  stands for the electric dipole-length operator, where  $\mu_0=0$  for linearly polarized light with its electric vector pointing along the  $z$  axis in the LAB frame, and  $\mu_0=\pm 1$  for circularly polarized light that propagates along the  $z$  axis in the LAB frame. We can express the dipole-length operator that appears in Eq. (26) in terms of the spherical harmonics defined in the MF frame

$$\sum_s r_s Y_{1\mu_0}(\hat{r}'_s) = \sum_s r_s \sum_{\mu} D_{\mu_0\mu}^{1*}(\hat{R}) Y_{1\mu}(\hat{r}'_s). \quad (27)$$

Combining expressions in Eqs. (24) through (27), we obtain

$$\begin{aligned}
& \langle \Psi_{p^+ \nu^+ N^+ \Lambda^+ M^+; \mathbf{k}'} | D_{\mu_0} | \Psi_{p \nu N \Lambda M_N} \rangle \\
& = \left( \frac{4\pi}{3} \right)^{1/2} \frac{1}{8\pi^2} (2N+1)^{1/2} (2N^++1)^{1/2} \sum_{lm\lambda\mu} i^{-l} e^{i\sigma_l} Y_{lm}(\hat{k}') \int d\Omega D_{M^+\Lambda^+}^{N^+}(\hat{R}) D_{m\lambda}^l(\hat{R}) D_{\mu_0\mu}^{1*}(\hat{R}) D_{M_N\Lambda}^{N^*}(\hat{R}) \\
& \quad \times \int dR \chi_{\nu^+}(R) [\langle \psi_{l\lambda}(\mathbf{r}; k, R) | \langle p^+ \Lambda^+ | \tilde{\mathbf{A}} \rangle \sum_s r_s Y_{1\mu}(\hat{r}'_s) | p \Lambda \rangle \chi_{\nu}(R)]. \quad (28)
\end{aligned}$$

The first integral in Eq. (28) can be evaluated readily using standard angular momentum algebra,<sup>45</sup> and the result can be found in the literature<sup>11,27</sup>

$$\begin{aligned}
& \int d\Omega D_{M^+\Lambda^+}^{N^+}(\hat{R}) D_{m\lambda}^l(\hat{R}) D_{\mu_0\mu}^{1*}(\hat{R}) D_{M_N\Lambda}^{N^*}(\hat{R}) \\
& = \sum_{N_t} 8\pi^2 (2N_t+1) \\
& \quad \times (-1)^{M^+-\mu_0+\Lambda^+-\mu} \begin{pmatrix} N & N^+ & N_t \\ M_N & -M^+ & M_t \end{pmatrix} \\
& \quad \times \begin{pmatrix} l & 1 & N_t \\ -m & \mu_0 & -M_t \end{pmatrix} \begin{pmatrix} N & N^+ & N_t \\ \Lambda & -\Lambda^+ & \Lambda_t \end{pmatrix} \\
& \quad \times \begin{pmatrix} l & 1 & N_t \\ -\lambda & \mu & -\Lambda_t \end{pmatrix}. \quad (29)
\end{aligned}$$

Here,  $N_t$  designates the angular momentum transferred between the photoelectron and the ion with  $M_t$  and  $\Lambda_t$  denoting its projections along the LAB frame and the MF-frame  $z$  axes, respectively,

$$\mathbf{N}_t = \mathbf{N}^+ - \mathbf{N} = \mathbf{1} - \mathbf{1}. \quad (30)$$

The last integral in Eq. (28) represents the vibrationally averaged electronic dipole-moment matrix element that connects the ionizing state to the continuum partial wave with angular momentum quantum number  $l$  and its projection on the internuclear axis  $\lambda$ .<sup>11,27,30</sup> We designate it as  $r_{l\lambda} e^{i\eta_{l\lambda}}$

$$\begin{aligned}
r_{l\lambda} e^{i\eta_{l\lambda}} & = \int dR \chi_{\nu^+}(R) [\langle \psi_{l\lambda}(\mathbf{r}; k, R) | \langle p^+ \Lambda^+ | \tilde{\mathbf{A}} \rangle \\
& \quad \times \sum_s r_s Y_{1\mu}(\hat{r}'_s) | p \Lambda \rangle \chi_{\nu}(R)]. \quad (31)
\end{aligned}$$

Under the independent electron approximation, Eq. (31) is simplified to a one-electron integral<sup>1</sup>

$$\begin{aligned}
r_{l\lambda} e^{i\eta_{l\lambda}} & = \int dR \chi_{\nu^+}(R) \\
& \quad \times \langle \psi_{l\lambda}(\mathbf{r}; k, R) | r Y_{1\mu}(\hat{r}) | \gamma(\mathbf{r}) \rangle \chi_{\nu}(R). \quad (32)
\end{aligned}$$

In Eq. (32),  $\mathbf{r}$  is the coordinate of the electron being ionized, and  $\gamma(\mathbf{r})$  is a one-electron orbital of that electron in the ionizing state. By inserting Eq. (19) into Eq. (32), we can express  $r_{l\lambda} e^{i\eta_{l\lambda}}$  in terms of the continuum eigenchannel quantities

$$\begin{aligned}
r_{l\lambda} e^{i\eta_{l\lambda}} & = \sum_{\alpha_\lambda} \int dR \chi_{\nu^+}(R) U_{l\alpha_\lambda}^\lambda e^{i\pi\tau_{\alpha_\lambda}^\lambda} \langle \xi_{\alpha_\lambda}^\lambda(\mathbf{r}; k, R) | r \\
& \quad \times Y_{1\mu}(\hat{r}) | \gamma(\mathbf{r}) \rangle \chi_{\nu}(R). \quad (33)
\end{aligned}$$

As noted in the previous section, the continuum quantities  $U_{l\alpha_\lambda}^\lambda$  and  $\tau_{\alpha_\lambda}^\lambda$  are dependent on the internuclear distance  $R$  and formally cannot be taken outside the integral. When the  $R$  dependence of continuum quantities  $U_{l\alpha_\lambda}^\lambda$  and  $\tau_{\alpha_\lambda}^\lambda$  is small and smooth over the range of  $R$  where the overlap between  $\chi_{\nu^+}(R)$  and  $\chi_{\nu}(R)$  is significant, Eq. (33) can be written as

$$r_{l\lambda} e^{i\eta_{l\lambda}} = \sum_{\alpha_\lambda} \bar{U}_{l\alpha_\lambda}^\lambda e^{i\pi\tau_{\alpha_\lambda}^\lambda} M_{\alpha_\lambda}^\lambda, \quad (34)$$

where

$$M_{\alpha_\lambda}^\lambda \equiv \int dR \chi_{\nu^+}(R) \langle \xi_{\alpha_\lambda}^\lambda(\mathbf{r}; k, R) | r Y_{1\mu}(\hat{r}) | \gamma(\mathbf{r}) \rangle \chi_{\nu}(R). \quad (35)$$

Here,  $M_{\alpha_\lambda}^\lambda$  represents the vibrationally averaged electronic dipole-moment matrix element that connects the ionizing electronic orbital to the  $\alpha_\lambda$ th continuum molecular orbital for each  $\lambda$ . It is important to note that  $M_{\alpha_\lambda}^\lambda$  is real because the radial parts of electronic wave functions are real and also because the vibrational wave functions are chosen to be real. In Eq. (34),  $\bar{U}_{l\alpha_\lambda}^\lambda$  and  $\bar{\tau}_{\alpha_\lambda}^\lambda$  are the representative values of  $U_{l\alpha_\lambda}^\lambda$  and  $\tau_{\alpha_\lambda}^\lambda$ , respectively, over that range of  $R$  where the vibrational overlap is significant. The equality in Eq. (34) is exact if  $U_{l\alpha_\lambda}^\lambda$  and  $e^{i\pi\tau_{\alpha_\lambda}^\lambda}$  are monotonically varying functions in this range of  $R$ , in which case  $\bar{U}_{l\alpha_\lambda}^\lambda$  and  $\bar{\tau}_{\alpha_\lambda}^\lambda$  can be chosen by the mean-value theorem.<sup>46</sup> Otherwise, the equality should be considered an approximation (reminiscent of the Franck–Condon approximation for bound–bound transitions), and  $\bar{U}_{l\alpha_\lambda}^\lambda$  and  $\bar{\tau}_{\alpha_\lambda}^\lambda$  can be taken as the vibrationally averaged values of  $U_{l\alpha_\lambda}^\lambda$  and  $\tau_{\alpha_\lambda}^\lambda$ , respectively. The approximation that the variations of  $U_{l\alpha_\lambda}^\lambda$  and  $\tau_{\alpha_\lambda}^\lambda$  with  $R$  are small and smooth is physically reasonable when we consider the direct photoionization of a bound state with small vibrational quanta. This approximation is likely to break down, however, when some dynamical phenomena, such as a shape resonance, occurs in molecular photoionization. It can be seen from Eq. (34) that the matrix  $\bar{\mathbf{U}}^\lambda$ , which is the vibrationally averaged version of the electronic transformation matrix  $\mathbf{U}^\lambda$ , acts as a unitary matrix that causes the rotation between two complex dipole lengths,  $\mathbf{r}_\lambda = \{r_{l\lambda} e^{i\eta_{l\lambda}}\}$  and  $\mathbf{M}^\lambda = \{M_{\alpha_\lambda}^\lambda e^{i\pi\tau_{\alpha_\lambda}^\lambda}\}$ .

Equations (34) and (35) are the key results of this analysis. These equations are important because they express the separation of the dipole-moment matrix elements that govern the photoionization dynamics into two parts: the quantities that are the properties of the continuum wave functions only, and the quantities that depend on both the ionizing state and the ionization continuum. In atomic and molecular physics, extensive experimental work has been performed to determine either continuum-related quantities (such as quantum defects determined from Rydberg spectroscopy) or quantities that depend both on the ionizing state and the continuum (such as electric dipole-moment matrix elements determined from photoelectron spectroscopy). For atomic photoionization, the relationship between these two types of quantities has been used extensively to interpret various experimental findings in a unified fashion.<sup>15,16,18–22</sup> It has also been shown that both the dipole-moment matrix elements and the scattering matrix elements can be extracted by combining various experimental data.<sup>17,34,47,48</sup> In molecular photoionization, however, systematic attempts to relate experimental findings in photoionization with collisional parameters are rare<sup>11</sup> despite the close relationship between electron–ion collision and photoionization, which has long been realized in the MQDT framework. This rarity stems from experimental and theoretical complexities inherent to the molecular problem. For instance, whereas the partial waves *are* the collision eigenchannels in atomic photoionization in the central-field approximation, this situation is not the case in molecules as discussed in the previous section. Equation (34) permits us to

extract detailed dynamical information pertaining to the ionization continuum from molecular photoionization experiments.

By inserting Eqs. (29) and (34) into Eq. (28), we obtain an expression for the transition electric-dipole matrix element

$$\begin{aligned} \langle \Psi_{p^+ \nu^+ N^+ \Lambda^+ M^+}; \mathbf{k}' | D_{\mu_0} | \Psi_{p\nu N\Lambda M_N} \rangle \\ = \left( \frac{4\pi}{3} \right)^{1/2} (2N+1)^{1/2} (2N^++1)^{1/2} \sum_{lm\lambda} \\ \times (-i)^l e^{i\sigma_l} Y_{lm}(\hat{\mathbf{k}}') \sum_{\alpha_\lambda} \bar{U}_{l\alpha_\lambda}^\lambda e^{i\pi\tau_{\alpha_\lambda}^\lambda} M_{\alpha_\lambda N_t \mu}^\lambda \sum_{\mu_0} \\ \times (-1)^{\mu_0 + \Lambda^+} C(l\lambda m N_t M_N \mu), \end{aligned} \quad (36)$$

where we define

$$\begin{aligned} C(l\lambda m N_t M_N \mu) \equiv (-1)^{\mu + M^+} (2N_t + 1) \begin{pmatrix} N & N^+ & N_t \\ M_N & -M^+ & M_t \end{pmatrix} \\ \times \begin{pmatrix} l & 1 & N_t \\ -m & \mu_0 & -M_t \end{pmatrix} \begin{pmatrix} N & N^+ & N_t \\ \Lambda & -\Lambda^+ & \Lambda_t \end{pmatrix} \\ \times \begin{pmatrix} l & 1 & N_t \\ -\lambda & \mu & -\Lambda_t \end{pmatrix}. \end{aligned} \quad (37)$$

The 3- $j$  symbols given in Eq. (37) determine the selection rules for the bound–free transitions when both the intermediate and the final states are described by Hund’s case (b) coupling. Because photoionization selection rules for various Hund’s coupling cases have already been discussed in the literature,<sup>49,50</sup> we do not discuss them explicitly here.

Note that in Eq. (36), the summations over  $l$  and  $\alpha_\lambda$  can be truncated at some finite value (see Appendix A). The summations over  $m$  and  $\lambda$ , which are quantum numbers related to  $l$ , are also truncated accordingly. The corresponding summations in the partial-wave expansion of the continuum wave function are not restricted in Eq. (12). Because of the light mass of the electron, the centrifugal barrier associated with the electronic motion near the ion core is very large, and the penetration of the photoelectron into the ion-core region is negligibly small when  $l$  is large. On the other hand, the electron density of the bound electronic orbital is concentrated in the ion-core region. In addition, the single-center expansion of tightly bound molecular orbitals usually shows rapid convergence with  $l$ . Consequently, the integrals in Eq. (32) become negligible when  $l$  is very large. Because the  $\xi_{\alpha_\lambda}^\lambda(\mathbf{r}; k, R)$  and the  $\psi_{l\lambda}(\mathbf{r}; k, R)$  are related to each other by the unitary transformation  $\mathbf{U}^\lambda$ ,  $\alpha_\lambda$  is also restricted when  $l$  is restricted.

The intensity of photoelectrons, or the rate of ejection of photoelectrons, associated with the ionization event  $|p^+ \nu^+ N^+ \Lambda^+ \rangle \leftarrow |p\nu N\Lambda \rangle$  and detected in the LAB-frame solid angle element  $d\Omega = \sin\theta d\theta d\phi$  is given by<sup>27,30</sup>

$$\begin{aligned}
I(\theta, \phi) = & 2\pi\alpha_{\text{fs}}F\hbar\omega \sum_{M^+} \sum_{M_N M'_N} \langle \Psi_{p^+ \nu^+ N^+ \Lambda^+ M^+; \mathbf{k}'} | \\
& \times D_{\mu_0} | \Psi_{p\nu N \Lambda M_N} \rangle \\
& \times \langle \Psi_{p\nu N \Lambda M'_N} | D_{\mu_0} | \Psi_{p^+ \nu^+ N^+ \Lambda^+ M^+; \mathbf{k}'} \rangle \rho_{M_N M'_N}^N.
\end{aligned} \quad (38)$$

Here,  $\alpha_{\text{fs}}$  is the fine structure constant,  $F$  represents the photon flux of light with frequency  $\omega$ , and  $\rho_{M_N M'_N}^N$  designates elements of the density matrix for the ionizing state<sup>51</sup> that specifies not only the populations of the different  $M_N$  sub-levels of a given  $N$  level in the ionizing state but also the coherences between these levels. Because we consider the photoionization from a specific quantum level in the ionizing state, the summation over  $N$  is omitted in Eq. (38). For an isotropic ensemble,  $\rho_{M_N M'_N}^N$  is simply given by

$$\rho_{M_N M'_N}^N = \frac{1}{2N+1} \delta_{M_N M'_N}. \quad (39)$$

When  $(n+1)$  REMPI is employed to study the photoionization from a specific quantum level in the intermediate state, the specific form of  $\rho_{M_N M'_N}^N$  for the intermediate state depends on the experimental geometry. Various forms of  $\rho_{M_N M'_N}^N$  can be found in the literature for different methods by which the ionizing state is reached.<sup>11,27,30</sup> Inserting Eq. (36) into Eq. (38) we obtain

$$\begin{aligned}
I(\theta, \phi) = & \frac{8\pi^2\alpha_{\text{fs}}}{3} F\hbar\omega \sum_{lm\lambda} \sum_{l'm'\lambda'} \gamma_{N^+ lm\lambda l' m' \lambda'} \\
& \times Y_{lm}(\hat{\mathbf{k}}') Y_{l'm'}^*(\hat{\mathbf{k}}') \sum_{\alpha_\lambda \alpha'_\lambda} \bar{U}_{l\alpha_\lambda}^\lambda \bar{U}_{l'\alpha'_\lambda}^{\lambda'} M_{\alpha_\lambda}^\lambda \\
& \times M_{\alpha'_\lambda}^{\lambda'} e^{i[\pi(\bar{\tau}_{\alpha_\lambda}^\lambda - \bar{\tau}_{\alpha'_\lambda}^{\lambda'}) + \sigma_l - \sigma_{l'}]},
\end{aligned} \quad (40)$$

where

$$\begin{aligned}
\gamma_{N^+ lm\lambda l' m' \lambda'} = & (2N+1)(2N^++1)(-i)^{l-l'} \\
& \times \sum_{M^+} \sum_{M_N M'_N} \sum_{N_t N'_t} \sum_{\mu\mu'} \\
& \times C(l\lambda m N_t M_N \mu) \\
& \times C(l'\lambda' m' N'_t M'_N \mu') \rho_{M_N M'_N}^N.
\end{aligned} \quad (41)$$

In Eq. (40),  $I(\theta, \phi)$  can be recast in terms of the spherical harmonics using the Clebsch–Gordan series<sup>27,45</sup>

$$I(\theta, \phi) = \sum_{L=\text{even}} \sum_M \beta_{LM} Y_{LM}(\theta, \phi), \quad (42)$$

where

$$\begin{aligned}
\beta_{LM} = & \frac{8\pi^2\alpha_{\text{fs}}}{3} F\hbar\omega \sum_{lm\lambda} \sum_{l'm'\lambda'} (-1)^m \\
& \times \left[ \frac{(2l+1)(2l'+1)(2L+1)}{4\pi} \right]^{1/2} \begin{pmatrix} l & l' & L \\ -m & m' & M \end{pmatrix} \\
& \times \begin{pmatrix} l & l' & L \\ 0 & 0 & 0 \end{pmatrix} \gamma_{N^+ lm\lambda l' m' \lambda'} \sum_{\alpha_\lambda \alpha'_\lambda} \bar{U}_{l\alpha_\lambda}^\lambda \bar{U}_{l'\alpha'_\lambda}^{\lambda'} M_{\alpha_\lambda}^\lambda \\
& \times M_{\alpha'_\lambda}^{\lambda'} e^{i[\pi(\bar{\tau}_{\alpha_\lambda}^\lambda - \bar{\tau}_{\alpha'_\lambda}^{\lambda'}) + \sigma_l - \sigma_{l'}]}.
\end{aligned} \quad (43)$$

In Eq. (43),  $\beta_{LM}$  depends not only on the magnitudes of electronic dipole-moment matrix elements,  $M_{\alpha_\lambda}^\lambda$ , but also on the scattering phase shifts,  $\bar{\tau}_{\alpha_\lambda}^\lambda$  and  $\sigma_l$ . Whereas  $U_{l\alpha_\lambda}^\lambda$  and  $\tau_{\alpha_\lambda}^\lambda$  can be assumed to be independent of energy, as discussed in the previous section, the Coulomb basis functions and  $\sigma_l$  have a nontrivial dependence on the asymptotic photoelectron energy  $\epsilon$ . The value of  $\beta_{LM}$  is, however, much less sensitive to  $\epsilon$  for two reasons. In contrast to their behavior at the asymptotic region,  $f_l$  and  $g_l$  are quite insensitive to  $\epsilon$  near the ion core.<sup>28</sup> Thus  $M_{\alpha_\lambda}^\lambda$ , whose magnitude stems mostly from the ion-core region, is insensitive to  $\epsilon$  in most cases. Also, whereas  $\sigma_l$  itself is strongly dependent on  $\epsilon$ ,  $\sigma_l - \sigma_{l'}$  does not vary rapidly with  $\epsilon$ . Using the properties of the gamma function and Stirling's approximation,<sup>28</sup> it can be shown that

$$\sigma_l - \sigma_{l'} = -\frac{\pi}{2}(l-l') + \frac{k}{2}(l-l')(l+l'+1) + O(k^2). \quad (44)$$

For most small diatomic ions,  $k$  varies typically less than 0.01 a.u. over the energy span of a few rotational levels within the same vibrational manifold. Hence,  $M_{\alpha_\lambda}^\lambda$  and  $\sigma_l$  remain approximately the same for different ion rotational levels within the same vibrational manifold. The form of the PAD for a given quantum level of the ion, which is described by  $\beta_{LM}$ , can also be approximated to be independent of energy over an energy range on the order of 100 meV.

## IV. DISCUSSION

We have derived in this article an expression for the quantum-state-specific PADs from direct photoionization of a diatomic molecule based on the molecular-orbital decomposition of the ionization continuum. The resulting expression for the quantum-state-specific PADs is dependent on two distinct types of dynamical quantities, one that pertains to the ionization continuum and the other that depends both on the ionizing state and the ionization continuum;  $\bar{U}_{l\alpha_\lambda}^\lambda$  and  $\bar{\tau}_{\alpha_\lambda}^\lambda$  can be classified as the former, whereas  $M_{\alpha_\lambda}^\lambda$  clearly belongs to the latter. Because  $\bar{U}_{l\alpha_\lambda}^\lambda$  and  $\bar{\tau}_{\alpha_\lambda}^\lambda$  describe only the dynamics in the ionization continuum, they should be common in photoionization processes from different ionizing states when the asymptotic photoelectron energy and the rovibronic state of the ion are the same. Hence, the present formalism allows for the maximal exploitation of the com-

monality between different photoionization processes in describing the direct photoionization of a molecule. The present formalism also enables the experimental investigation of the ionization continuum by studying quantum-state-specific PADs.

It is straightforward to employ the expression derived here to predict experimental PADs based on the dynamical quantities obtained from theoretical calculations. It has been shown that the dynamical quantities that pertain to the molecular ionization continuum, as well as the dipole-moment matrix elements that couple an ionizing state to the ionization continuum, can be found in *ab initio* calculations within the independent electron approximation.<sup>41,52–56</sup> Once these *ab initio* results are available, they can be substituted into the expressions given in this article to yield quantum-state-specific photoionization cross sections and PADs associated with each quantum level of the ion.

Equations (42) and (43) can also be used to fit experimental PADs to obtain the dynamical parameters  $M_{\alpha_\lambda}^\lambda$ ,  $\bar{U}_{l\alpha_\lambda}^\lambda$ , and  $\bar{\tau}_{\alpha_\lambda}^\lambda$ . The quantum-state-specific PADs from a single electronic state of a molecule are not, however, sufficient to retrieve all the dynamical parameters that appear in Eq. (43). As shown in our previous report of the complete quantum-mechanical description for the photoionization of the NO  $A^2\Sigma^+(\nu=0)$  state,<sup>10–12</sup> magnitudes and phases of the electronic dipole-moment matrix elements that connect a given ionizing state to each partial wave in the ionization continuum, which are designated as  $r_{l\lambda}$  and  $\eta_{l\lambda}$ , respectively, in Eq. (31), completely specify the photoionization dynamics from the ionizing state. The dynamical parameters in the present formalism,  $M_{\alpha_\lambda}^\lambda$ ,  $\bar{U}_{l\alpha_\lambda}^\lambda$ , and  $\bar{\tau}_{\alpha_\lambda}^\lambda$ , contain, on the other hand, information on the dynamics in the ionization continuum in addition to dynamical information on the photoionization from a given ionizing state. Consequently, whereas we can uniquely determine  $r_{l\lambda}$  and  $\eta_{l\lambda}$  from  $M_{\alpha_\lambda}^\lambda$ ,  $\bar{U}_{l\alpha_\lambda}^\lambda$ , and  $\bar{\tau}_{\alpha_\lambda}^\lambda$  using Eq. (34), the reverse is not possible.

One solution for this indeterminacy is to use the information obtained from the spectroscopy of high-lying Rydberg states in fitting experimental PADs and reduce the number of fitting parameters. As discussed in Sec. II,  $\bar{U}_{l\alpha_\lambda}^\lambda$  and  $\bar{\tau}_{\alpha_\lambda}^\lambda$  can be approximated by the Rydberg-series mixing coefficients and the electronic quantum defects of high-lying Rydberg states, respectively,<sup>44</sup> assuming that we ignore their weak energy dependence and provided that the vibrational quantum number of the Rydberg states is the same as that of the residual ion produced after photoionization. Under these conditions, the remaining dynamical parameters in the fit are only a set of real parameters,  $M_{\alpha_\lambda}^\lambda$ , which can then be uniquely determined from quantum-state-specific PADs from a single ionizing state. From a practical standpoint, this fit is easier to perform than the fit of experimental PADs with  $r_{l\lambda}$  and  $\eta_{l\lambda}$  as fitting parameters. Admittedly, however, this method works only when the approximation is valid that  $\bar{U}_{l\alpha_\lambda}^\lambda$  and  $\bar{\tau}_{\alpha_\lambda}^\lambda$  are energy independent and when the spectroscopic data are available for high-lying Rydberg states.

The more satisfactory solution to obtain all the dynamical

parameters in Eq. (43) is to fit simultaneously quantum-state-specific PADs from two or more electronic states. As emphasized repeatedly, the ionization continuum reached from different photoionization processes is the same as long as the asymptotic photoelectron energy and the rovibronic state of the ion produced are the same. Thus  $\bar{U}_{l\alpha_\lambda}^\lambda$  and  $\bar{\tau}_{\alpha_\lambda}^\lambda$  should be the same for photoionization processes from different electronic states when the above conditions are met, whereas  $M_{\alpha_\lambda}^\lambda$  is specific for a given electronic state being ionized. Consequently, the number of independent parameters in the simultaneous fit of experimental PADs from multiple electronic states increases much more slowly than the number of independent data points in the fit, which makes possible the unique determination of all the dynamical parameters necessary to specify the photoionization dynamics of multiple electronic states *and* the dynamics in the ionization continuum. This procedure is illustrated in the companion article for the photoionization of the NO  $A^2\Sigma^+(\nu=0)$  and  $D^2\Sigma^+(\nu=0)$  states.<sup>31</sup>

In this study, we have derived a theoretical expression for quantum-state-specific PADs from direct photoionization of a diatomic molecule in which both the ionizing state and the state of the ion follow Hund's case (b) coupling. The present formalism, which is based on the independent electron approximation, can be compared to the "single-channel" partial-wave formalism for atomic photoionization (see Sec. II and Table II)<sup>29</sup> and should be regarded as the starting point for theoretical improvements to include more complex photoionization phenomena. It nevertheless provides a unified description for the direct photoionization of a diatomic molecule that explicitly incorporates the molecular nature of the problem. It also provides a theoretical framework for the experimental study of the dynamics in the molecular ionization continuum.

It is relatively straightforward to extend the present formalism to the photoionization of a diatomic molecule that follows other Hund's coupling cases by employing one-electron continuum wave functions that explicitly account for the electron spin.<sup>57</sup> The present formalism can also be generalized to describe photoionization of polyatomic molecules using the final-state one-electron wave functions that depend on molecular geometry. For linear molecules, the formalism presented in this article can be directly extended provided that the ion is also linear. For symmetric-top molecules,  $\lambda$  in the present formalism should be interpreted as the projection of  $l$  on the molecular figure axis.<sup>58</sup> The one-electron continuum wave function for a symmetric-top molecule should be symmetry adapted,<sup>59,60</sup> as is the bound molecular orbital.

To describe various autoionization phenomena, the more general MQDT formalism that explicitly accounts for the closed channel contribution should be employed.<sup>24,26,61</sup> In this case, however, the concept of a one-electron orbital that parametrically depends on the molecular geometry should be discarded because the breakdown of the Born–Oppenheimer approximation in the asymptotic region should be fully taken into account.

## ACKNOWLEDGMENTS

H.P. is grateful for a Franklin Veatch Memorial Fellowship from Stanford University. We acknowledge the support of the National Science Foundation under Grant No. PHY-9320356.

## APPENDIX A: SCATTERING MATRICES

In this Appendix, we discuss the specific form of various scattering matrices that appears in the main text. As discussed in Sec. III, the summations in Eq. (36) can be truncated. In theoretical calculations, the value of maximum  $l$  in the summation,  $l_{\max}^{\lambda}$ , can be determined by variational stability of the summations as a function of the number of  $l$  channels included.<sup>14</sup> The value of  $l_{\max}^{\lambda}$  can also be determined from the maximum  $\Delta N (= N^{+} - N)$  observed in the rotationally resolved photoelectron spectrum based on the angular momentum constraints.<sup>8</sup> In photoionization of most small molecules for which the energy of the asymptotic photoelectron is less than 2 eV, the inclusion of up to  $f(l=3)$  or  $g(l=4)$  waves in the ionization continuum is shown to be sufficient to explain experimental data.<sup>9,11-13,62,63</sup>

The value of  $l_{\max}^{\lambda}$  determines the sizes of various scattering matrices because the number of partial-wave channels involved in the scattering process for a given  $\lambda$  is given by  $l_0^{\lambda} \equiv l_{\max}^{\lambda} - |\lambda|$ . The MF-frame scattering matrix  $\mathbf{S}^{\lambda}$  and the MF-frame reaction matrix  $\mathbf{K}^{\lambda}$  are  $l_0^{\lambda} \times l_0^{\lambda}$  matrices. The electronic transformation matrix  $\mathbf{U}^{\lambda}$  is also an  $l_0^{\lambda} \times l_0^{\lambda}$  matrix. Geometrically,  $\mathbf{U}^{\lambda}$  is an  $l_0^{\lambda} \times l_0^{\lambda}$  orthogonal matrix that describes a rotation in  $l_0^{\lambda}$ -dimensional space.<sup>47</sup> Because a rotation in the  $l_0^{\lambda}$ -dimensional space can be decomposed into a combination of the  $b_{\max}^{\lambda} \equiv l_0^{\lambda}(l_0^{\lambda}-1)/2$  elementary rotations, we can write  $\mathbf{U}^{\lambda}$  in the following form:

$$\mathbf{U}^{\lambda} = \prod_{b^{\lambda}=1}^{b_{\max}^{\lambda}} \mathbf{R}_{b^{\lambda}}^{\lambda}(\vartheta_{b^{\lambda}}^{\lambda}). \quad (\text{A1})$$

Here,  $b^{\lambda}$  is an index defined by the following convention:

$$b^{\lambda} = \begin{matrix} 1 & 2 & \cdots & l_0^{\lambda}-1 & l_0^{\lambda} & \cdots & b_{\max}^{\lambda} \\ (l, l') = & (|\lambda|, |\lambda|+1) & (|\lambda|, |\lambda|+2) & \cdots & (|\lambda|+1, |\lambda|+2) & \cdots & (l_{\max}-1, l_{\max}) \end{matrix} \quad (\text{A2})$$

and

$$\mathbf{R}_{b^{\lambda}}^{\lambda}(\vartheta_{b^{\lambda}}^{\lambda}) = \begin{pmatrix} & (1) & (2) & \cdots & (i) & \cdots & \cdots & (j) & \cdots & (l_0^{\lambda}) \\ (1) & 1 & 0 & \cdots & 0 & \cdots & \cdots & 0 & \cdots & 0 \\ (2) & 0 & 1 & 0 & \vdots & \cdots & \cdots & \vdots & \cdots & \vdots \\ \vdots & \vdots & 0 & \ddots & \vdots & \cdots & \cdots & \vdots & \cdots & \vdots \\ (i) & 0 & \cdots & \cdots & \cos \vartheta_{b^{\lambda}}^{\lambda} & 0 & \cdots & \sin \vartheta_{b^{\lambda}}^{\lambda} & \cdots & 0 \\ \vdots & \vdots & \cdots & \cdots & 0 & 1 & \cdots & 0 & \cdots & \vdots \\ \vdots & \vdots & \cdots & \cdots & \vdots & \cdots & \ddots & \vdots & \cdots & \vdots \\ (j) & 0 & \cdots & \cdots & -\sin \vartheta_{b^{\lambda}}^{\lambda} & 0 & \cdots & \cos \vartheta_{b^{\lambda}}^{\lambda} & \cdots & 0 \\ \vdots & \vdots & \cdots & \cdots & \vdots & \cdots & \cdots & \vdots & \ddots & \vdots \\ (l_0^{\lambda}) & 0 & \cdots & \cdots & 0 & \cdots & \cdots & 0 & \cdots & 1 \end{pmatrix}. \quad (\text{A4})$$

Here,  $\vartheta_{b^{\lambda}}^{\lambda}$  stands for the mixing angle between the  $i$ th and the  $j$ th partial-wave channels for each value of  $\lambda$ .

## APPENDIX B: RELATIONSHIP BETWEEN OUR FORMALISM AND MQDT

In this Appendix, we discuss the equivalence of the formalism presented in this article to the so-called ‘‘open-continuum’’ MQDT.<sup>39</sup> Instead of showing the equivalence by rederiving the expression for quantum-state-specific PADs from MQDT, we point out here that the theoretical elements of the MQDT can indeed be retrieved from our formalism. Specifically, we show that various frame transformation matrix elements that are central in the molecular MQDT formulation<sup>25</sup> can be found in our expressions. The rest of the proof relies on angular momentum coupling algebra that involves the coupling of the ionizing photon and the molecule.

In molecular MQDT, the asymptotic ionization channels are related to the short-range eigenchannels by a set of frame transformations, that is, the electronic, vibrational, and rotational frame transformations.<sup>24,25</sup> In the discussion of molecular Rydberg spectroscopy and various autoionization phenomena, introduction of the frame transformation has proven especially beneficial because it allows for the description of complex rovibrational interactions among Rydberg levels in terms of a few short-range eigenchannel quantities.<sup>26</sup> For the direct photoionization that is the subject of the present study, however, the concept of the frame transformation is not as significant.

The electronic frame transformation matrix is represented in our formalism by the matrix  $\mathbf{U}^{\lambda}$ . The vibrational frame transformation matrix elements are the vibrational wave functions of the ion,  $\chi_{v^{+}}(R)$ . The rotational frame transformation matrix elements are contained in the first in-

tegral of Eq. (28), as can be shown by writing the integral as

$$\int d\Omega D_{M^+\Lambda^+}^{N^+}(\hat{R})D_{m\lambda}^l(\hat{R})D_{\mu_0\mu}^1 *(\hat{R})D_{M_N\Lambda}^N *(\hat{R})$$

$$= \sum_{JM_J\Lambda_J} 8\pi^2(2J+1) \begin{pmatrix} N^+ & l & J \\ M^+ & m & M_J \end{pmatrix} \begin{pmatrix} N^+ & l & J \\ \Lambda^+ & \lambda & \Lambda_J \end{pmatrix}$$

$$\times \begin{pmatrix} 1 & N & J \\ \mu_0 & M_N & M_J \end{pmatrix} \begin{pmatrix} 1 & N & J \\ \mu & \Lambda & \Lambda_J \end{pmatrix}. \quad (\text{B1})$$

Evaluation of the integral can be performed by using the Clebsch–Gordan series<sup>45</sup>

$$D_{M^+\Lambda^+}^{N^+}(\hat{R})D_{m\lambda}^l(\hat{R}) = \sum_{JM_J\Lambda_J} (2J+1) \begin{pmatrix} N^+ & l & J \\ M^+ & m & M_J \end{pmatrix}$$

$$\times \begin{pmatrix} N^+ & l & J \\ \Lambda^+ & \lambda & \Lambda_J \end{pmatrix} D_{M_J\Lambda_J}^{J*}(\hat{R}), \quad (\text{B2})$$

$$D_{\mu_0\mu}^1 *(\hat{R})D_{M_N\Lambda}^{N*}(\hat{R}) = \sum_{JM_J\Lambda_J} (2J+1) \begin{pmatrix} 1 & N & J \\ \mu_0 & M_N & M_J \end{pmatrix}$$

$$\times \begin{pmatrix} 1 & N & J \\ \mu & \Lambda & \Lambda_J \end{pmatrix} D_{M_J\Lambda_J}^J(\hat{R}), \quad (\text{B3})$$

and Eq. (3.113) of Ref. 45. Here,  $\mathbf{J}$  is the total angular momentum of the photoionization process (excluding nuclear and electronic spin) defined by

$$\mathbf{J} = \mathbf{N}^+ + \mathbf{I} = \mathbf{N} + \mathbf{1}, \quad (\text{B4})$$

with  $M_J$  and  $\Lambda_J$  denoting its projections along the  $z$  axes of the LAB frame and MF frame, respectively. The equivalence of Eq. (B1) and Eq. (29) in Sec. III can be shown readily through a pair of recoupling transformations.<sup>45</sup> In Eq. (B1), the second  $3-j$  symbol corresponds to the rotational frame transformation matrix elements without parity adaptation.<sup>25</sup> The rotational frame transformation matrix elements signify the transformation between the MF-frame and the LAB-frame representations of the composite state of the ion and the photoelectron, or equivalently, the change in representation between Hund's case (b) and (d) coupling.

<sup>1</sup>K. Wang, J. A. Stephens, and V. McKoy, *J. Phys. Chem.* **97**, 9874 (1993).

<sup>2</sup>I. Cacelli, V. Carvetta, A. Rizzo, and R. Moccia, *Phys. Rep.* **205**, 283 (1991).

<sup>3</sup>W. G. Wilson, K. S. Viswanathan, E. Sekreta, and J. P. Reilly, *J. Phys. Chem.* **88**, 672 (1984).

<sup>4</sup>S. T. Pratt, P. M. Dehmer, and J. L. Dehmer, *J. Chem. Phys.* **85**, 3379 (1986).

<sup>5</sup>E. W. Schlag, W. B. Peatman, and K. Müller-Dethlefs, *J. Electron Spectrosc.* **66**, 139 (1993).

<sup>6</sup>F. Merkt and T. P. Softley, *Int. Rev. Phys. Chem.* **12**, 205 (1993).

<sup>7</sup>J. Xie and R. N. Zare, *Chem. Phys. Lett.* **159**, 399 (1989).

<sup>8</sup>S. W. Allendorf, D. J. Leahy, D. C. Jacobs, and R. N. Zare, *J. Chem. Phys.* **91**, 2216 (1989).

<sup>9</sup>D. J. Leahy, K. L. Reid, and R. N. Zare, *J. Chem. Phys.* **95**, 1757 (1991).

<sup>10</sup>K. L. Reid, D. J. Leahy, and R. N. Zare, *Phys. Rev. Lett.* **68**, 3527 (1992).

<sup>11</sup>D. J. Leahy, K. L. Reid, H. Park, and R. N. Zare, *J. Chem. Phys.* **97**, 4948 (1992).

<sup>12</sup>H. Park and R. N. Zare, *J. Chem. Phys.* **99**, 6537 (1993).

<sup>13</sup>H. Park and R. N. Zare, *Chem. Phys. Lett.* **225**, 327 (1994).

<sup>14</sup>H. Rudolph and V. McKoy, *J. Chem. Phys.* **91**, 2235 (1989).

<sup>15</sup>J. Cooper and R. N. Zare, in *Lectures in Theoretical Physics*, edited by S. Geltman, K. T. Mahanthappa, and W. E. Brittin (Gordon and Breach, New York, 1969), Vol. XI-C, p. 317.

<sup>16</sup>J. C. Hansen, J. J. A. Duncanson, R. -L. Chien, and R. S. Berry, *Phys. Rev. A* **21**, 222 (1980).

<sup>17</sup>U. Heinzmann, *J. Phys. B* **13**, 4367 (1980).

<sup>18</sup>H. Kaminski, J. Kessler, and J. Kollath, *Phys. Rev. Lett.* **45**, 1161 (1980).

<sup>19</sup>O. C. Mullins, R. Chien, J. E. H. III, J. S. Keller, and R. S. Berry, *Phys. Rev. A* **31**, 321 (1985).

<sup>20</sup>S. J. Smith and G. Leuchs, *Adv. At. Mol. Phys.* **24**, 157 (1988).

<sup>21</sup>A. Hausmann, B. Kämmerling, H. Kossmann, and V. Schmidt, *Phys. Rev. Lett.* **61**, 2669 (1988).

<sup>22</sup>Y. -Y. Yin and D. S. Elliott, *Phys. Rev. A* **47**, 2881 (1993).

<sup>23</sup>U. Fano, *Phys. Rev. A* **2**, 353 (1970).

<sup>24</sup>C. H. Greene and Ch. Jungen, *Adv. At. Mol. Phys.* **21**, 51 (1985).

<sup>25</sup>E. S. Chang and U. Fano, *Phys. Rev. A* **6**, 173 (1972).

<sup>26</sup>Ch. Jungen and O. Atabek, *J. Chem. Phys.* **66**, 5584 (1977).

<sup>27</sup>K. L. Reid, D. J. Leahy, and R. N. Zare, *J. Chem. Phys.* **95**, 1746 (1991).

<sup>28</sup>M. J. Seaton, *Rep. Prog. Phys.* **46**, 167 (1983).

<sup>29</sup>U. Fano and A. R. P. Rau, *Atomic Collisions and Spectra* (Academic, Orlando, 1986).

<sup>30</sup>S. N. Dixit and V. McKoy, *J. Chem. Phys.* **82**, 3546 (1985).

<sup>31</sup>H. Park and R. N. Zare, *J. Chem. Phys.* **104**, 4568 (1996).

<sup>32</sup>V. L. Jacobs, *J. Phys. B* **5**, 2257 (1982).

<sup>33</sup>S. Ross, in *Proceedings of AIP Conference, Caracas, Venezuela, 1990*, edited by M. Garcia-Sucre, G. Raseev, and S. C. Ross (American Institute of Physics, New York, 1990), p. 73.

<sup>34</sup>K. T. Lu, *Phys. Rev. A* **4**, 579 (1971).

<sup>35</sup>R. Shankar, *Principles of Quantum Mechanics* (Plenum, New York, 1980).

<sup>36</sup>A. D. Buckingham, B. J. Orr, and J. M. Sichel, *Philos. Trans. R. Soc. London, Ser. A* **268**, 147 (1970).

<sup>37</sup>G. Breit and H. A. Bethe, *Phys. Rev.* **93**, 888 (1954).

<sup>38</sup>D. Dill and J. L. Dehmer, *J. Chem. Phys.* **61**, 692 (1974).

<sup>39</sup>Ch. Jungen and D. Dill, *J. Chem. Phys.* **73**, 3338 (1980).

<sup>40</sup>N. F. Mott and H. S. W. Massey, *The Theory of Atomic Collisions*, 3rd ed. (Clarendon, Oxford, 1965).

<sup>41</sup>M. Brosolo and P. Decleva, *Chem. Phys.* **159**, 185 (1992).

<sup>42</sup>R. G. Newton, *Scattering Theory of Waves and Particles* (McGraw-Hill, New York, 1966).

<sup>43</sup>D. Loomba, S. Wallace, D. Dill, and J. L. Dehmer, *J. Chem. Phys.* **75**, 4546 (1981).

<sup>44</sup>S. Fredin, D. Gauyacq, M. Horani, Ch. Jungen, G. Lefevre, and F. Masnou-Seeuws, *Mol. Phys.* **60**, 825 (1987).

<sup>45</sup>R. N. Zare, *Angular Momentum* (Wiley-Interscience, New York, 1988).

<sup>46</sup>T. M. Apostol, *Mathematical Analysis*, 2nd ed. (Addison-Wesley, Amsterdam, 1981).

<sup>47</sup>C. -M. Lee and K. T. Lu, *Phys. Rev. A* **8**, 1241 (1973).

<sup>48</sup>Z. -W. Wang and K. T. Lu, *Phys. Rev. A* **31**, 1515 (1985).

<sup>49</sup>S. N. Dixit and V. McKoy, *Chem. Phys. Lett.* **128**, 49 (1986).

<sup>50</sup>J. Xie and R. N. Zare, *J. Chem. Phys.* **93**, 3033 (1990).

<sup>51</sup>K. Blum, *Density Matrix Theory and Applications* (Plenum, New York, 1981).

<sup>52</sup>R. R. Lucchese and V. McKoy, *Phys. Rev. A* **24**, 770 (1981).

<sup>53</sup>J. -M. Li and K. L. Vo, *Commun. Theor. Phys.* **2**, 1175 (1983).

<sup>54</sup>K. Kaufmann, C. Nager, and M. Jungen, *Chem. Phys.* **95**, 385 (1985).

<sup>55</sup>J. A. Stephens and V. McKoy, *J. Chem. Phys.* **97**, 8060 (1992).

<sup>56</sup>I. Cacelli, R. Moccia, and A. Rizzo, *J. Chem. Phys.* **98**, 8742 (1993).

<sup>57</sup>K. Wang and V. McKoy, *J. Chem. Phys.* **95**, 4977 (1991).

<sup>58</sup>D. J. Leahy, K. L. Reid, and R. N. Zare, *J. Phys. Chem.* **95**, 8154 (1991).

<sup>59</sup>P. G. Burke, N. Chandra, and F. A. Gianturco, *J. Phys. B* **5**, 2212 (1972).

<sup>60</sup>N. Chandra, *J. Phys. B* **20**, 3405 (1987).

<sup>61</sup>D. Dill, *Phys. Rev. A* **6**, 160 (1972).

<sup>62</sup>K. Wang, J. A. Stephens, V. McKoy, E. de Beer, C. A. de Lange, and N. P. C. Westwood, *J. Chem. Phys.* **97**, 211 (1992).

<sup>63</sup>J. A. Stephens and V. McKoy, *J. Chem. Phys.* **93**, 7863 (1990).